Submitted to International Journal of Fatigue – December 2020
(Special Issue of VAL4 Conference)

Confidence interval of the 'single-moment' fatigue damage calculated from an estimated power spectral density

D. Benasciutti*

Department of Engineering, University of Ferrara, via Saragat 1, 44122, Ferrara, Italy

Abstract. This article develops a theoretical approach to account for the uncertainty of the fatigue damage caused by the sampling variability of a power spectral density estimated from a finite length stationary record. The moment generating function of the estimated spectral moments is obtained and used to approximate their probability distribution with that of a chi-square random variable with a newly chosen number of degrees of freedom. This approximate distribution allows the confidence interval of both the 'true' spectral moments and 'single-moment' damage to be derived. A numerical example is finally presented to demonstrate the correctness of the proposed solutions.

Keywords

Random loading; power spectral density; spectral moments; 'single-moment' damage; sampling variability

* Denis Benasciutti
E-mail: denis.benasciutti@unife.it
Phone: +39 0532 974976, Fax: +39 0532 974870

Highlights

- fatigue damage from an estimated power spectral density is statistically uncertain
- moment generating function of the estimated spectral moments is obtained
- confidence interval for the 'true' spectral moments
- confidence interval for the damage by the 'single-moment' spectral method

Nomenclature

C, k	parameters of the S-N curve
D_{NB}	'true' narrow-band damage
D_{SM}	'true' single-moment damage
$\widehat{D}_{NB}$	estimated narrow-band damage
$\widehat{D}_{SM}$	estimated 'single-moment' damage
f	frequency
Δf	frequency resolution
$G(f)$	'true' power spectral density
$\hat{G}(f)$	estimated power spectral density
K	number of segments (blocks) in $x(t)$
m_q	'true' spectral moment of order q
$\widehat{m}_q$	estimated spectral moment of order q
$M(\theta)$	moment generating function
n	number of degrees of freedom
r	overlap ratio
T	total time length of $x(t)$
T_s	segment time length
$x(t)$	sample realisation of time length T
$\{x(t)\}$	random process
$(1-\alpha)$	confidence
ε_r	normalised random error
v_q	equivalent degrees of freedom
$\hat{v}_q$	estimated equivalent degrees of freedom
χ^2_n	chi-square random variable with n dof
$\chi^2_{n;x}$	x-percentage point of chi square random variable
dof	degrees of freedom
edof	equivalent degrees of freedom
mgf	moment generating function
pdf	probability density function

1. Introduction

The durability analysis of structures undergoing random loadings can be addressed in the frequency-domain by the use of spectral methods. After characterising a random loading by its power spectral density (PSD), spectral methods provide mathematical expressions that allow the fatigue damage to be estimated from combinations of PSD spectral parameters.

A great many spectral methods exist in the literature. Starting from the pioneering works of Miles [1] and Bendat [2], so many spectral methods have been proposed that it would be almost impossible to mention them all here. Some examples, in chronological order, are found in [3-10]. The great majority of spectral methods apply to stationary random loadings with Gaussian or non-Gaussian probability distribution. In fact, the variety of non-stationarities encountered in practical applications makes rather hard to develop a spectral model encompassing any type of non-stationary loading, though solutions exist for specific subclasses [11,12,13].

A feature common to all spectral methods is that they consider the power spectral density as being a 'true' quantity, known exactly without any statistical uncertainty. This situation is purely hypothetical, as in practice things go differently. Usually the power spectral density is estimated from one or more measured records and therefore it only represents an estimate of the true but unknown power spectral density [14]. This estimate has an intrinsic statistical variability that transfers to all quantities (e.g. the damage) computed from it.

The importance of the statistical variability of an estimated power spectrum and its spectral parameters seems to be well known in the field of ocean engineering [15-19]. But surprisingly it has received no attention in the field of structural durability, where the statistical variability characterising the fatigue damage computed from an estimated power spectrum is not considered by spectral methods. Developing a theoretical approach by which to quantify such a statistical variability of the damage constitutes the purpose of this article, which represents an extended version of [20].

To make things more specific, let a random loading be represented as a stationary and ergodic random process $\{x(t)\}$, $-\infty < t < \infty$. The process represents an infinite collection (or ensemble) of time-histories $x(t)$ of unlimited time length T. Given only one sample record $x(t)$, the one-sided power spectral density of $\{x(t)\}$ is defined as [14,21]:

$$G(f) = 2 \lim_{T\to\infty} \frac{1}{T} E[\,|X(f,T)|^2\,] \tag{1}$$

where $E[-]$ denotes the expected value and $X(f,T)$ indicates the finite Fourier Transform of $x(t)$:

$$X(f,T) = \int_0^T x(t) e^{-j2\pi f t}\, dt \tag{2}$$

where symbol j is the imaginary unit and e is the natural exponent. The power spectrum $G(f)$ so defined embodies, in the frequency-domain, the main statistical properties of the random process $\{x(t)\}$ (e.g. variance, rate of mean value up-crossings, rate of peaks, peak distribution) [22].

A random process is classified depending on whether its power spectrum is narrow-band or wide-band. If $G(f)$ is clustered over a very narrow frequency interval, process $\{x(t)\}$ is called narrow-band, whereas if $G(f)$ is spread over a wider frequency interval the process is called wide-band.

For a narrow-band Gaussian process, the expected damage per second (damage intensity) is [2]:

$$D_{NB} = \frac{2^{k/2}}{C} \Gamma\left(1 + \frac{k}{2}\right) m_0^{\frac{k-1}{2}} m_2^{1/2} \tag{3}$$

in which $\Gamma(-)$ is the gamma function, and m_0, m_2 are the zero- and second-order spectral moments [22,23]:

$$m_q = \int_0^\infty (2\pi f)^q G(f) df \qquad (q = 1,2,\dots) \tag{4}$$

(f is the frequency in Hertz). Symbols C and k define the S-N curve $s^k N_f = C$, relating the number of cycles to failure N_f to the stress amplitude s in a constant amplitude loading. Parameters k and C are usually estimated by a regression analysis of experimental fatigue data and their statistical variability is not considered here.

In the circumstance in which the random process is wide-band, Eq. (3) is too conservative and other damage expressions should be used. Some examples can be found in [6,9]. For the

discussion that follows, it is useful to recall the 'singe-moment' method as it has the advantage to relate the damage to a single spectral moment: [4,5]:

$$D_{SM} = \frac{2^{k/2}}{2\pi C}\left(m_{2/k}\right)^{k/2}\Gamma\left(1+\frac{k}{2}\right) \tag{5}$$

Despite its simplicity, this method was proved to agree well with time-domain results in the case of power spectral densities ranging from narrow-band to wide-band [4,5,6].

It has to be emphasised that the expected damage in Eq. (3) and (5) adopts an S-N curve with constant slope and no fatigue limit, also known as elementary Miner's rule [25,25].

Whichever spectral method is considered, the damage always depends upon one or more spectral moments m_q of the power spectral density. Therefore, the power spectral density and its spectral moments play a key role in the calculation of the damage in the frequency-domain. That being said, the cases in which the power spectral density is expressed by a mathematical formula are rare, apart from a few exceptions (e.g. ISO standard for road roughness [26], Pierson-Moskowitz for fully developed waves [27], von Karman-Harris for atmospheric turbulence [28], just to name a few). In these fortunate cases, one can use the power spectrum expression directly, or as input in a spectral dynamic analysis aimed at determining the output stress power spectra at any point in a linear structure.

In all other less fortunate cases, the power spectral density must be estimated from one or more measured time-history records of finite time length. In the Welch's method [29], for example, the power spectral density comes from averaging the power spectra of overlapped segments into which a sample record has been divided. Methods other than Welch's are also available [30].

Any method will nevertheless provide only an estimate of the 'true' power spectrum in Eq. (1), which can never be computed exactly. Indeed, the 'true' power spectrum is a mathematical idealisation because – as stated by Eq. (1) – it would require an infinite number of infinite-length records, which are never available in practice. On the other hand, the 'true' PSD can be bounded by a confidence interval constructed from a PSD estimated from an observed time-history record. The estimated power spectrum is a sample realisation of the 'true' power spectrum. The difference between the two constitutes the sampling variability (or statistical uncertainty) of the estimated power spectrum.

What is more important for a structure durability analysis is that the statistical uncertainty of an estimated power spectrum transfers to its spectral moments and, in turn, to the fatigue damage computed by Eq. (3) or (5), or by any other expression. Both the spectral moments and the damage – if coming from an estimated power spectrum – are themselves sample values with an inherent statistical uncertainty. Quantifying this statistical uncertainty then becomes of paramount importance.

This goal will be achieved as follows. Starting from the chi-square distribution followed by an estimated power spectral density, the article obtains the moment generating function (mgf) of the spectral moments. This mgf is used to approximate the probability distribution of spectral moments with a scaled chi-square random variable. This result allows the confidence interval of the spectral moments of any order to be easily derived. This result then serves to derive the confidence interval of the 'single-moment' spectral fatigue damage.

2. Power spectral density estimated from a finite-length record

The power spectral density $G(f)$ defined in Eq. (1) represents the 'true' spectrum of the random process $\{x(t)\}$. It is clearly a mathematical abstraction, as requires an ensemble averaging over all possible realisations of infinite duration that belong to $\{x(t)\}$.

In practice, one has available only few records of finite duration – if not perhaps only one. These records only allow for an estimate of the 'true' power spectral density, which thus remains unknown. For example, given one sample stationary record $x(t)$ of time length T, an estimate of $G(f)$ is obtained by omitting the limiting and expectation operations in Eq. (1) [14]:

$$\hat{G}(f) = \frac{2}{T}|X(f,T)|^2 \tag{6}$$

Throughout the text, $\hat{G}(f)$ will be named as sample, or estimated, power spectral density to distinguish it from the 'true' power spectral density $G(f)$.

Unlike $G(f)$, the sample power spectrum $\hat{G}(f)$ is defined at discrete and equally spaced frequencies f_i. The frequency resolution $\Delta f = f_{i+1} - f_i$ is the distance between adjacent points and it is determined by the total record length, $\Delta f = 1/T$. The spectral values $\hat{G}(f_i)$,

$i = 1, \ldots, N$ are independent [16]. The number of points in the power spectrum, $N = n_p/2 + 1$, is established by the number of points n_p that form the digitalised version of $x(t)$ [14].

It can be demonstrated that, at each frequency, the spectral estimate $\hat{G}(f)$ is distributed as a chi-square random variable with n =2 degrees of freedom (dof) [14]:

$$\frac{\hat{G}(f)}{G(f)} = \frac{\chi_2^2}{2} \tag{7}$$

The power spectrum estimated in this way has a rather large standard deviation, as large as the 'true' power spectrum being estimated [14]. The standard deviation can be reduced by increasing the number of dofs. To this end, the original record $x(t)$ is divided into K adjacent disjoint segments (or blocks) of equal length T_s, see Figure 1(a); the power spectral density of $x(t)$ is estimated by averaging the power spectra of each segment (Welch's technique) [14,29]. With this record subdivision, the frequency resolution is established by the segment length, $\Delta f = 1/T_s$, see Figure 1(b), and the previous relationship becomes [14]:

$$\frac{\hat{G}(f)}{G(f)} = \frac{\chi_n^2}{n} \qquad (n = 2K) \tag{8}$$

At each frequency, the spectral estimate $\hat{G}(f)$ is used to construct a confidence interval for the true but unknown spectral value $G(f)$. The fact that the ratio $\frac{n\hat{G}(f_i)}{G(f_i)} = \chi_n^2$ is a chi-square random variable allows writing the following probability statement:

$$Pr\left\{\chi_{n;1-\alpha/2}^2 \leq \frac{n\hat{G}(f_i)}{G(f_i)} \leq \chi_{n;\alpha/2}^2\right\} = 1 - \alpha \tag{9}$$

where $\chi_{n;x}^2$ is the x-percentage point of the chi-square distribution with n dofs, whose values are tabulated in statistics textbooks [14,31].

After rearranging the quantities inside the brackets, the previous expression turns into the $(1-\alpha)$ confidence interval that bounds the true but unknown spectral value $G(f)$ [14]:

$$\frac{n\hat{G}(f)}{\chi_{n;\alpha/2}^2} \leq G(f) \leq \frac{n\hat{G}(f)}{\chi_{n;1-\alpha/2}^2} \tag{10}$$

For example, for n=10 and $(1-\alpha) = 0.95$, it is $\chi_{n;0.025}^2$=20.48 and $\chi_{n;0.975}^2$=3.25, which yields the two limits 0.488 and 3.077 for the ratio $G(f)/\hat{G}(f)$. Based on these limits, one may

conclude that, given a value of $\hat{G}(f)$ at every frequency, the true power spectral value $G(f)$ is not known to within a factor of ~6.3 at the 95% confidence level.

The approach described so far and depicted in Figure 1 conveys the main idea lying behind the power spectrum estimated from a measured record. In practice, data windowing and segment overlapping are often used to improve the power spectrum estimate [14,23,32]. Data windowing (e.g. Hanning window) alleviates the "frequency leakage"; segment overlapping raises the number of dofs by further increasing the number of segments in a single record. These improvement techniques, on the other hand, tends to weak the validity of the chi-square distribution for the estimated spectrum [23] and are not considered hereafter. Nevertheless, not considering these aspects does by no means undermine the validity of the approach presented in the following.

A further aspect to be emphasised is that the time-history record $x(t)$ being analysed needs to be stationary for the PSD to exist. Quite often this requirement is violated in practical applications, where measured vibration data are everything but exactly stationary [12,33,34]. When the standard estimation procedures are applied anyway, they may yield an enormous scatter of the possible results depending on the chosen parameters of analysis. For example, large differences may be observed from analysing longer or shorter segments of a measured record that, on the whole, is markedly non-stationary [34]. In such circumstances, the deviations arising from longer or shorter stationary (or almost stationary) records – which represent the inherent statistical scatter of a PSD – are small in comparison with the deviations from analysing signals that violate the requirements of a PSD estimation.

3. Confidence interval for sample spectral moments

This section introduces the concept of sample spectral moments for an estimated power spectral density and develops an approach for estimating their probability distribution. The section concludes by defining the confidence interval of the 'true' spectral moments.

3.1. Sample spectral moments

Since $G(f)$ is a continuous function of frequency, its spectral moment m_q of order q is defined in Eq. (4) as an integral over all frequencies. By contrast, the estimated spectrum

$\hat{G}(f_i)$, $i = 1, \dots, N$ is defined at N discrete frequency points f_i, so its spectral moments are approximated by a summation:

$$\widehat{m}_q = \sum_{i=1}^{N} \left[(2\pi f_i)^q \hat{G}(f_i) \Delta f \right] \qquad (q = 1,2, \dots) \tag{11}$$

Using Eq. (8) and introducing the coefficient $a_i = (2\pi f_i)^q \frac{G(f_i)}{n} \Delta f$, the previous expression becomes:

$$\widehat{m}_q = \sum_{i=1}^{N} a_i \chi_n^2 \tag{12}$$

where $a_i \chi_n^2$ is a multiple of a chi-square random variable, with scale parameter a_i and n degrees of freedom. Equation (12) shows that $\widehat{m}_q$ is a weighted linear combination of chi-square random variables with a common number of dofs n, but different parameters a_i, $i = 1, \dots, N$. Therefore, $\widehat{m}_q$ is a random variable, too.

The 'hat' symbol emphasises that $\widehat{m}_q$ is an estimate of the true but unknown spectral moment m_q; it represents a sample value of m_q. Note that taking the expected value of $\widehat{m}_q$ does not remove the summation $E\left[\widehat{m}_q\right] = \Delta f \sum_{i=1}^{N} (2\pi f_i)^q G(f_i)$ and, therefore, represents an approximation of the "integral" spectral moment m_q. This result occurs because the frequency axis remains divided into discrete values f_i, with a resolution $\Delta f = 1/T_s$ controlled by the segment length. Only in the limit $T_s \to \infty$ would the frequency axis become continuous and the summation converge to an integral.

3.2. Moment generating function and probability distribution of sample spectral moments

This section obtains the moment generating function of $\widehat{m}_q$, which is next used to approximate the corresponding probability density function. The moment generating function (mgf) of a random variable Z is defined as [31]:

$$M(\theta) = E\left[e^{\theta z}\right] = \int_{-\infty}^{\infty} e^{\theta z} f_Z(z) dz \tag{13}$$

provided that the integral exists. The mgf is the Laplace transform of the probability density function $f_Z(z)$ of Z. A mgf is an equivalent way to express a probability density function, which – in principle – can be retrieved as the inverse Laplace transform of its mgf [31].

A useful property of $M(\theta)$ is that its derivatives computed at $\theta = 0$ return the moments of $f_Z(z)$ about the origin. For example, the first and second derivatives yield the first and second moments:

$$E[Z] = \left.\frac{dM}{d\theta}\right|_{\theta=0} \qquad E[Z^2] = \left.\frac{d^2M}{d\theta^2}\right|_{\theta=0} \tag{14}$$

The variance is $Var(Z) = E[Z^2] - (E[Z])^2$; symbol $E[Z^2]$ denotes the "expected value of Z squared" and $(E[Z])^2$ denotes the "square of the expected value of Z".

While textbooks often report the formulae of $M(\theta)$ for the most common probability distributions (Gaussian, Rayleigh,…) [31], for the scaled chi-square random variable $a\chi_n^2$ the mgf is [35,36]:

$$M_{a\chi_n^2}(\theta) = (1 - 2a\theta)^{-\frac{n}{2}} \qquad \text{for} \quad \theta < \frac{1}{2a} \tag{15}$$

At this point, it is useful to define the mgf $M_{\widehat{m}_q}(\theta) = E\left[e^{\theta \widehat{m}_q}\right]$ for the random variable $\widehat{m}_q$. Substituting the expression given in Eq. (12):

$$M_{\widehat{m}_q}(\theta) = E\left[exp\left(\theta \sum_{i=1}^{N} a_i \chi_n^2\right)\right] = E\left[\prod_{i=1}^{N} e^{\theta a_i \chi_n^2}\right] \tag{16}$$

where the second equality follows from the property $exp(\theta \sum_i^N c_i) = \prod_{i=1}^N e^{\theta c_i}$. The previous expression can be further elaborated. Since the random variables $a_i\chi_n^2$, $i = 1, \dots, N$ are independent, the expected value of their product equals the product of their expected values:

$$E\left[\prod_{i=1}^{N} e^{\theta a_i \chi_n^2}\right] = \prod_{i=1}^{N} E\left[e^{\theta a_i \chi_n^2}\right] \tag{17}$$

The quantity $M_{a_i\chi_n^2}(\theta) = E\left[e^{\theta a_i \chi_n^2}\right]$ represents the mgf of the chi-square random variable $a_i\chi_n^2$, as exemplified in Eq. (15). Substituting in Eq. (17), one gets the mgf of the sample spectral moment $\widehat{m}_q$:

$$M_{\widehat{m}_q}(\theta) = \prod_{i=1}^{N} (1 - 2a_i\theta)^{-\frac{n}{2}} \qquad \left(a_i = (2\pi f_i)^q \frac{G(f_i)}{n} \Delta f\right) \tag{18}$$

This product of moment generating functions is too complicated and cannot be inverted to obtain an analytical form for the probability distribution of $\widehat{m}_q$. However, this product of mgfs can be approximated by the mgf of a chi-square random variable, say $Y = c\chi_v^2$, with a newly chosen parameter c and number of dofs v. This approach corresponds to approximating the probability distribution of $\widehat{m}_q$ with the probability distribution of Y.

The goal is to determine c and v. More precisely, the approximation seeks those values of c and v for which the expected value and the variance of $\widehat{m}_q$ and Y are equal:

$$\begin{aligned} E[Y] &= E\left[\widehat{m}_q\right] \\ Var(Y) &= Var\left[\widehat{m}_q\right] \end{aligned} \tag{19}$$

This approximation is often credited to Satterthwaite [37]. The random variable Y has expected value $E[Y] = cv$ and variance $Var(Y) = 2c^2v$ [38]. Solving for c and v:

$$v = \frac{2(E[Y])^2}{Var[Y]} \qquad c = \frac{Var[Y]}{2E[Y]} \tag{20}$$

As established by the previous approximation, the expected value and variance of Y are to be replaced by those of $\widehat{m}_q$:

$$v = \frac{2\left(E\left[\widehat{m}_q\right]\right)^2}{Var\left(\widehat{m}_q\right)} \qquad c = \frac{Var\left(\widehat{m}_q\right)}{2E\left[\widehat{m}_q\right]} \tag{21}$$

where $Var(\widehat{m}_q) = E\left[\widehat{m}_q^2\right] - \left(E\left[\widehat{m}_q\right]\right)^2$. The first and second moments, $E\left[\widehat{m}_q\right]$ and $E\left[\widehat{m}_q^2\right]$, are now determined from the first and second derivatives of $M_{\widehat{m}_q}(\theta)$ computed at $\theta = 0$. The Appendix A summarises the main mathematical steps; the final expressions of the expected value and variance of $\widehat{m}_q$ are:

$$E\left[\widehat{m}_q\right] = n\sum_{i=1}^{N} a_i \qquad Var\left(\widehat{m}_q\right) = 2n\sum_{i=1}^{N} a_i^2 \tag{22}$$

Substituting these two expressions in Eq. (21), and the definition of $a_i = (2\pi f_i)^q \frac{G(f_i)}{n}\Delta f$, one gets the final expression of υ:

$$\upsilon_q = \frac{n\left[\sum_{i=1}^{N} f_i^q G(f_i)\right]^2}{\sum_{i=1}^{N}\left[f_i^q G(f_i)\right]^2} \tag{23}$$

(the expression of c is omitted being of no interest for the following discussion).

For $q = 0$, the quantity υ_0 is often called the "equivalent degrees of freedom" (edof) of the power spectral density $G(f_i)$ [16,17].

Some features of υ_q are worth to be highlighted. As clear from Eq. (23), the quantity υ_q is a function of several parameters. It is proportional to the number of dofs n, which equals the number of segments K. It has also to be noticed that, in the sums of Eq. (23), the true power spectrum $G(f_i)$ is to be computed at the same discrete frequencies f_i, $i = 1, \ldots, N$ in which also the estimated power spectrum is defined. This definition makes υ_q inversely proportional to the frequency resolution Δf that controls how many points N define the discrete frequency axis.

The parameter υ_q also depends both on the order q of the spectral moment (a subscript is added, indeed) and on the shape of the power spectral density. This last dependence is demonstrated in Figure 2, which compares υ_0 for four different power spectral shapes. The value υ_0 is independent of the actual values of $G(f_i)$. For the special case of $G(f_i)$=const. over the whole set of discrete frequencies, Eq. (23) becomes $\upsilon_0 = nN$; this value represents an upper bound for υ_0.

In the sum in Eq. (23), each term $f_i^q G(f_i)$ is actually not known, because it is a function of the true power spectrum $G(f_i)$. If $G(f_i)$ is replaced by its estimate $\hat{G}(f_i)$, Eq. (23) gives the sample estimate $\hat{\upsilon}_q$ corresponding to υ_q.

3.3. Confidence interval for the true spectral moment

According to the procedure described so far, the sample spectral moment $\hat{m}_q$ is approximated by a scaled chi-square random variable $\hat{m}_q = c\chi^2_{\hat{\upsilon}_q}$, with $\hat{\upsilon}_q$ degrees of freedom and parameter c. Its expected value is $E\left[\hat{m}_q\right] = c\hat{\upsilon}_q$.

The dependence on c can be made to disappear. Considering that $E[\hat{m}_q] \cong m_q$ (this result has already been commented above), it is possible to write the scale parameter as $c = m_q/\hat{v}_q$ and substitute it into the definition of $\hat{m}_q$, which shows that the ratio $\frac{\hat{v}_q \hat{m}_q}{m_q} = \chi^2_{\hat{v}_q}$ is a chi-square random variable with $\hat{v}_q$ dofs.

Exploiting the close similarity with $\frac{n\hat{G}(f_i)}{G(f_i)} = \chi^2_n$, it is possible to write the $(1-\alpha)$ confidence interval for the true spectral moment m_q:

$$\frac{\hat{v}_q\, \hat{m}_q}{\chi^2_{\hat{v}_q;\alpha/2}} \leq\ m_q \leq \frac{\hat{v}_q \hat{m}_q}{\chi^2_{\hat{v}_q;1-\alpha/2}} \tag{24}$$

where $\chi^2_{\hat{v}_q;x}$ is the x-percentage point of the chi-square distribution with $\hat{v}_q$ dofs.

In the special case $q = 0$, the previous equation gives the confidence interval for the variance (i.e. zero order spectral moment) of the random process:

$$\frac{\hat{v}_0 \hat{m}_0}{\chi^2_{\hat{v}_0;\alpha/2}} \leq\ m_0\ \leq \frac{\hat{v}_0 \hat{m}_0}{\chi^2_{\hat{v}_0;1-\alpha/2}} \tag{25}$$

where $\hat{m}_0 = \widehat{Var}(\{x(t)\})$ is the sample variance, corresponding to the area under the estimated power spectrum $\hat{G}(f)$. A similar result is quoted in [17,18] for the significant wave height $H_s = 4\sqrt{m_0}$.

4. Confidence interval of fatigue damage

It has already been emphasised that, in any spectral method, the fatigue damage explicitly depends on one or more spectral moments m_q of the power spectral density $G(f)$. An example is in Eq. (3) and (5). The power spectrum $G(f)$, its spectral moments m_q, and the damage computed from them, represent 'true' but unknown quantities as they characterise the countless set of realisations in the stationary random process $\{x(t)\}$.

When instead one single realization is considered, one obtains the power spectrum $\hat{G}(f)$ and its spectral moments $\hat{m}_q$ that represent estimates of $G(f)$ and m_q, respectively. The use of the estimates $\hat{m}_q$ yields an estimate of the 'true' fatigue damage. For example, Eq. (5) gives the estimate of the 'single-moment' damage as:

$$\hat{D}_{SM} = \frac{2^{k/2}}{2\pi C}\left(\hat{m}_{2/k}\right)^{k/2} \Gamma\left(1+\frac{k}{2}\right) \tag{26}$$

while the estimate of the narrow-band damage $\widehat{D}_{NB}$ follows after replacing, in Eq. (3), the true moments m_0, m_2 with their sample estimates $\widehat{m}_0$, $\widehat{m}_2$.

The quantities $\widehat{D}_{SM}$ and $\widehat{D}_{NB}$ represent the estimates of D_{SM} and D_{NB}. The estimates are two sample values with an intrinsic statistical uncertainty that comes from the sampling uncertainty in the power spectrum $\hat{G}(f)$ from which the damage is computed.

The statistical uncertainty of the damage can be evaluated through confidence intervals. It is, however, not trivial to obtain a confidence interval for the narrow-band damage in Eq. (3), as it combines m_0, m_2 in a nonlinear fashion (product, square root, exponentiation).

It is much easier to deal with the 'single-moment' damage as it only involves one spectral moment. To start with, consider the inequality in Eq. (24) for the special case $q = 2/k$. The inequality remains unchanged if each of its terms is first raised to the exponent $k/2$ and then multiplied by the constant $\frac{2^{k/2}}{2\pi C}\Gamma\left(1+\frac{k}{2}\right)$. Using Eq. (5) and (26), one finally obtains:

$$\left(\frac{\hat{\upsilon}_{2/k}}{\chi^2_{\hat{\upsilon}_{2/k};\,\alpha/2}}\right)^{k/2}\widehat{D}_{SM} \le D_{SM} \le \left(\frac{\hat{\upsilon}_{2/k}}{\chi^2_{\hat{\upsilon}_{2/k};\,1-\alpha/2}}\right)^{k/2}\widehat{D}_{SM} \qquad (27)$$

where D_{SM} is the true but unknown damage obtained from the true spectral moment $m_{2/k}$ in Eq. (5), and $\widehat{D}_{SM}$ the corresponding estimate from Eq. (26).

Symbol $\chi^2_{\hat{\upsilon}_{2/k};x}$ indicates the x-percentage point of the chi-square distribution with $\hat{\upsilon}_{2/k}$ dofs, where $\hat{\upsilon}_{2/k}$ is the equivalent dof of order $2/k$ computed by Eq. (23). Notice that the above confidence interval is a function of the power spectral density shape via the parameter $\hat{\upsilon}_{2/k}$.

The confidence interval in Eq. (27) can be used to bound the unknown single-moment damage D_{SM}, which characterises the infinite ensemble of time-histories of the stationary random process $\{x(t)\}$.

By contrast, the sample damage $\widehat{D}_{SM}$ depends on a particular sample time-history from which the power spectrum $\hat{G}(f)$ has been estimated. The damage value $\widehat{D}_{SM}$ thus incorporates the statistical uncertainty coming from the estimated power spectrum $\hat{G}(f)$.

A final aspect to be emphasised is that the approach presented so far is restricted to stationary random loadings. Whenever this requirement is not fulfilled exactly, errors are introduced in the estimated PSD that may be as large as, if not even larger than, the confidence bands of the damage calculated as above.

5. Numerical case study

5.1. The role of PSD estimation parameters

The estimated power spectrum $\hat{G}(f)$ represents one single realisation of the true but unknown power spectral density $G(f)$. At each frequency, the spectral estimate $\hat{G}(f)$ is a chi-square random variable with n degrees of freedom. This randomness of $\hat{G}(f)$ transfers to the spectral moment $\hat{m}_{2/k}$ and, in turn, to the single-moment damage $\widehat{D}_{SM}$.

Besides this, the estimated power spectrum $\hat{G}(f)$ provides only an approximate representation of $G(f)$. This approximation comes from the fact that $\hat{G}(f)$ is defined at discrete frequencies, whereas $G(f)$ is continuous; the distance between discrete frequencies is established by the frequency resolution $\Delta f = 1/T_s$.

The damage estimate $\widehat{D}_{SM}$ is then a function of n and Δf. Both parameters are considered in the numerical example illustrated in Section 5.2; its purpose is to study the statistical variability of $\widehat{D}_{SM}$ and to verify the correctness of Eq. (27).

In the practical calculation of a power spectral density, in which target levels of both statistical accuracy and spectral resolution must be achieved, parameters n and Δf cannot be chosen arbitrarily.

The statistical accuracy in power spectrum estimate is quantified by the normalised random error (coefficient of variation) $\varepsilon_r = \sqrt{2/n}$ [14]. A way to diminish ε_r is to increase the number of degrees of freedom n. In the Welch's method, this goal is obtained by increasing the number of records from which the power spectrum is averaged. A single time-history record is then subdivided into segments, each one contributing with 2 dofs. For K segments, it is $n = 2K$ and the normalised random error becomes $\varepsilon_r = 1/\sqrt{K}$ [14]. This definition demonstrates that ε_r decreases if the number of segments K is made to increase.

But K cannot increase indefinitely. If the total length T must be kept constant (for example, because a record has already been measured), an increase of K shortens the segment length T_s and broadens the frequency resolution $\Delta f = 1/T_s$. Moreover, subdividing a record into too short segments may affect the perception of the stationarity of the record itself, especially if the entire record is not exactly stationary. For example, too short values of T_s may enhance a local non-stationary character of record portions and then lead to classify the whole record as

being non-stationary. Also the choice of which portions of a non-stationary record need to be analysed is a critical task, as it may lead to different PSD estimations [33].

In case the total length is not bound to a fixed value, the frequency resolution becomes an additional degree of freedom allowed to be changed independently. Specifying the value of the frequency resolution determines the block length as $T_s = 1/\Delta f$. A narrow resolution requires a longer segment length, and therefore a longer total record length, too. For distinct blocks with no overlapping, the total record length is simply $T = KT_s$. Overlapping reduces this value. In this case, the total length is $T = [(K-1)(1-r)+1]T_s$, where r (from 0 to 1.0) is the overlap fraction between consecutive segments [23]. Higher ratios r (up to 75%) may be used to keep T within reasonable limits, in case a high number of segments K is required to achieve a low ε_r. Another way to decrease the frequency resolution artificially is by adding zeros at the end of the digitalised signals of every segment (zero padding) [32].

Table 1 clarifies the relationship among the parameters mentioned above, and how they change with the combinations of n and Δf used in the subsequent numerical simulations. The total length T refers to an overlapping fraction of r=0.50 and 0.75. Combining the highest number of segments with the narrowest frequency resolution gives the smallest error, but also the longest length T.

The values in Table 1 are merely indicative. They indeed assume that the record length T is the result of an arbitrary choice of n and Δf. Nevertheless, a too high value of T may not be achieved in practice. Often – if not almost always – it is only possible to measure one sample record of limited time length. In this case, conflicting requirements arise. For example, if the number of blocks is kept fixed to guarantee a certain estimation error ε_r, a reduction of the total duration T (and thus of the segment length T_s) would cause the frequency resolution Δf to increase. The estimated power spectrum would accordingly become smoother, but with a too broad frequency resolution the peaks in the power spectrum could not be detected precisely.

5.2. Numerical simulation procedure

The following numerical example encompasses a broad range of combinations of n and Δf. As the 'true' power spectral density, it considers the following expression [5,39]:

$$G(f) = A\frac{7793}{T_d^4(2\pi f)^5}\frac{exp[-1948/(T_d 2\pi f)^4]}{\left\{\left[1-\left(\frac{f}{f_n}\right)^2\right]^2+\left(2\xi\frac{f}{f_n}\right)^2\right\}} \quad (28)$$

in which A=scale factor, ξ=damping ratio, f_n=natural frequency of the fundamental mode of the structure, T_d=dominant wave period. Without loss of generality, the scale factor A is so adjusted that the power spectrum area is unity ($m_0 = 1$). The power spectral density is cut-off at a frequency f_c=1.5 Hz.

The previous equation is meant to approximate the stress power spectral density in offshore platforms; it modifies the Pierson-Moskowitz spectrum to incorporate the resonance effect, by treating an off-shore platform as a simple oscillator (which is an oversimplification that neglects interaction effects between different parts of the structure). Typical parameters values (T_d=5 sec, ξ=0.02, f_n=1.143 Hz) were chosen in the numerical simulations [39].

Simulations examined a total of 16 different combinations of the number of degrees of freedom, n, and of the frequency resolution Δf. Each parameter was assigned the values $n =$ 10, 30, 70, 150 and Δf= 0.005, 0.01, 0.02, 0.03 Hz.

For each of the 16 possible combinations of n and Δf, a total of 10000 power spectrum realisations $\hat{G}_l(f_i)$, $l = 1, \ldots, 10000$, were generated from the true power spectral density $G(f)$.

The following procedure was adopted [18]. The frequency resolution Δf established the distance between contiguous points in the frequency grid f_i, $i = 1, \ldots, N$ at which $\hat{G}_l(f_i)$ was defined. Each ordinate $\hat{G}_l(f_i)$ was evaluated independently from a chi-square random number generator, with expected value $G(f_i)$ and n degrees of freedom. As a result, each sample realisation $\hat{G}(f_i)$ took on discrete values defined on a frequency grid (with points at distance Δf) and following a chi-square distribution. As an example, Figure 3 compares the true power spectrum with two realisations corresponding to different combinations of Δf and n. The combination with higher n and lower Δf leads to the smaller estimation error (less scatter).

For each realisation of the power spectrum $\hat{G}_l(f_i)$, the analysis determined the sample spectral moment $\hat{m}_{2/k}$ and the equivalent dof $\hat{v}_{2/k}$, according to Eqs. (11) and (23), respectively. These quantities were next used to determine the sample damage $\hat{D}_{SM}$ by Eq. (26), and the

confidence interval by Eq. (27). The damage computation assumed an S-N curve with parameters k=3 and C=1.

In summary, for each combination of n and Δf, a total of 10000 sample values were generated for each of the random variables $\hat{m}_{2/k}$, $\hat{v}_{2/k}$ and $\widehat{D}_{SM}$. These observed samples values have been elaborated to estimate the frequency histograms that, suitably normalised, provided the probability density function (pdf).

Note that the number of discrete frequencies in each power spectrum realisation is $N = f_c/\Delta f$ and, for a given cut-off frequency, that number only depends on the frequency resolution. In numerical simulations, the number ranged from 50 (for Δf=0.03 Hz) to 300 (for Δf=0.005 Hz).

Different is the behaviour of $\hat{v}_{2/k}$. Not only does it indirectly depend on Δf through the positions of the discrete frequencies, but – as shown in Eq. (23) – it also depends on n and $\hat{G}_l(f_i)$. Being $\hat{v}_{2/k}$ a random variable, the previous dependence is best illustrated by considering the mean value of $\hat{v}_{2/k}$. For the combinations of Δf and n here scrutinised, the mean value varied from minimum of 126 (for Δf=0.03 Hz, n=10) up to a maximum of 12906 (for Δf=0.005 Hz, n=150).

5.3. Discussion of results

Figure 4 displays the pdfs of the single-moment damage for the sixteen combinations of n and Δf examined. The damage values are normalised to the expected (true) damage, as $\widehat{D}_{SM}/D_{SM}$. The unit value indicates the true damage; values other than unity characterise the sampling error in the damage estimate. Note that two different y-axis limits are set up so that the pdfs can adapt best to the space available in every subplot.

The figure reveals that the pdfs shape has a dual dependence on Δf and n. Some general trends are clear. For small Δf and large n, the spectral resolution is high and the normalised random error low. In this case, the probability distributions tend to narrow around the true value of the damage; this means that there is little sampling variability in the damage computed from the estimated power spectrum. This fortunate situation nevertheless requires a record with a very long duration (the longest one from those in Table 1).

As n decreases, the pdfs become broader – that is, the variance of the damage estimate increases. For almost all the combinations of Δf and n, the damage pdfs tend to be symmetric

around the expected value. They also approximate a normal distribution, despite the fact that the individual power spectral estimates from which the damage is computed follow a chi-square distribution.

As the frequency resolution increases, the degree by which the estimated power spectrum approximates the true power spectrum gets worse. Accordingly, an error is introduced in estimating the damage and the pdfs become broader. As both n and Δf increase, the spectral resolution progressively dominates over the statistical variability; the pdfs become more flatted and slightly asymmetric. In particular, the pdf shape tends to become not symmetric (slightly skewed to the left) for the combination having the lowest number of dofs and the highest frequency resolution.

The deviation from a symmetric shape is accompanied by a deviation from the normal distribution. This trend is confirmed by the comparison of the normal probability plots in Figure 5. The figure refers to the two opposite cases for which the equivalent degrees of freedom turns out to be, on average, the smallest and the highest, respectively.

The tendency of the sample damage to be normally distributed can be explained by the fact that, for high dofs (usually >100), a chi-square distribution asymptotically approaches a normal distribution [31].

The last result examined is the confidence interval of the damage. Figure 6 shows two examples of a subset of 25 (out of 10000) confidence intervals for the 'true' single-moment damage. The remaining intervals, being very similar to those shown, are not displayed to avoid making each figure too confused.

The intervals are constructed around the sample damage (solid circles) according to Eq. (27), for a confidence $(1-\alpha) = 0.950$. The sample damage is normalised as $\widehat{D}_{SM}/D_{SM}$. Although the figure refers to the cases n=10, Δf=0.03 Hz and n=70, Δf=0.01 Hz, other combinations lead to similar results. It is nevertheless interesting to note that the second combination, having a higher dof and smaller resolution, leads to a lower damage variability and narrower confidence intervals, see also Figure 4.

The results in Figure 6 allow one to check the correctness of Eq. (27). Indeed, by counting the number of confidence intervals (on a total of 10000) that enclose the 'true' damage it is possible to obtain the estimate $(1-\hat{\alpha})$ of the 'true' confidence value $(1-\alpha)$ associated with the confidence interval.

This counting was repeated for all the combinations n and Δf shown in Figure 4. The resulting values of estimated confidence are listed in the boxes in Figure 4, and also in the last column of Table 1.

The values of $(1-\hat{\alpha})$ fall in the range 0.950÷0.969; the highest values correspond to the lowest n. The estimated and the true confidence are almost coincident; the difference of only few percentage points is perfectly acceptable given the approximations in the proposed approach.

It has finally to be emphasised that larger values of $(1-\hat{\alpha})$ would result if the power spectrum realisations are generated with values of n and Δf lower than those used in Table 1. In particular, too large a value of Δf would introduce a crude – and thus unacceptable – sampling approximation of the true power spectrum shape; this would yield too large deviations between the true and the sample values of both spectral moments and damage, thus decreasing the accuracy of Eq. (27). This situation is enhanced in regions where the power spectral density exhibits sharp peaks, as in the example considered in this study. It is then recommended than the frequency resolution be carefully chosen to avoid the occurrence of such an approximation.

6. Conclusions

This work dealt with the sampling variability in power spectrum estimation and how it affects the fatigue damage computed by a frequency-domain approach. This sampling variability characterises a power spectral density that is estimated from a stationary time-history record of finite length. This represents the situation usually encountered in practice, where only few records – if not perhaps only one – are usually available from measurements.

The work first obtained the analytical expression of the moment generating function (mgf) of the sample spectral moments computed from an estimated power spectral density. This mgf expression allowed one to approximate the probability distribution of the sample spectral moments by a chi-square probability distribution with a newly chosen number of degrees of freedom (named "equivalent degrees of freedom" of the power spectral density). This result was next used to obtain the confidence interval expression for the sample spectral moments and, more importantly, for the fatigue damage computed by the 'single-moment' spectral

method. The obtained confidence interval expression provides a way to account for the sampling variability characterising the damage computed from an estimated power spectrum.

The correctness of the confidence interval expressions was verified through a numerical example, in which sixteen combinations of frequency resolution and number of degrees of freedom (dofs) were analysed. The number of dofs corresponds to twice the number of sub-segments used in the Welch's method for estimating the power spectral density from a time-history record.

The numerical example also provided an insight on how the probability density function of the sample damage varies as a function of the frequency resolution and the number of dofs, for the above sixteen combinations examined. The lowest statistical variability in the damage (that is, the lowest variance) occurs with the lowest frequency resolution and the highest number of dofs. This very desirable situation, however, requires a time-history record with a very long duration – yet not always achievable in practice. In this case, the equivalent degrees of freedom are very high, and the damage probability distribution approximates a normal distribution.

By contrast, when the frequency resolution increases and the number of dofs decreases, the probability distribution has a larger variance, meaning a larger statistical variability in the damage. At the same time, the probability distribution deviates from the normal distribution and becomes slightly skewed. The variance increases, too, meaning an increased statistical variability in the damage.

Nevertheless, the main conclusion of this study is that the fatigue damage computed – through spectral methods – from an estimated power spectral density has to be regarded as a sampling value inherently random, regardless of which specific combination of frequency resolution and number of dofs is considered in the power spectrum estimation.

7. Appendix: computation of the origin moments of sample spectral moments

This Appendix explains the result in Eq. (22); it is obtained from the first and second derivative of the mgf $M_{\widehat{m}_q}(\theta)$ in Eq. (18) of the random variable $\widehat{m}_q$.

It is much easier to consider a mgf with only two terms ($N = 2$):

$$M_{\widehat{m}_q}(\theta) = \prod_{i=1}^{2}(1 - 2a_i\theta)^{-\frac{n}{2}} = (1 - 2a_1\theta)^{-\frac{n}{2}}\,(1 - 2a_2\theta)^{-\frac{n}{2}} \tag{29}$$

The first derivative of $M_{\hat{m}_q}(\theta)$ is:

$$\frac{dM}{d\theta} = a_1 n(1-2a_1\theta)^{-\frac{n}{2}-1}\,(1-2a_2\theta)^{-\frac{n}{2}} + \; a_2 n(1-2a_1\theta)^{-\frac{n}{2}}\,(1-2a_2\theta)^{-\frac{n}{2}-1} \tag{30}$$

Deriving once more yields the second derivative:

$$\begin{aligned}\frac{d^2M}{d\theta^2} = {} & 2a_1^2 n\left(\frac{n}{2}+1\right)(1-2a_1\theta)^{-\frac{n}{2}-2}(1-2a_2\theta)^{-\frac{n}{2}} \\ & + 2a_1 a_2 n^2(1-2a_1\theta)^{-\frac{n}{2}-1}(1-2a_2\theta)^{-\frac{n}{2}-1} \\ & + 2a_2^2 n\left(\frac{n}{2}+1\right)(1-2a_1\theta)^{-\frac{n}{2}}(1-2a_2\theta)^{-\frac{n}{2}-2}\end{aligned} \tag{31}$$

There are two equal "cross terms" that add together.

The first derivative computed at $\theta = 0$ gives the first moment about the origin (expected value):

$$E\left[\hat{m}_q\right] = \left.\frac{dM}{d\theta}\right|_{\theta=0} = a_1 n + a_2 n = n(a_1 + a_2) \tag{32}$$

The second derivative computed at $\theta = 0$ gives the second moment about the origin (mean square value):

$$E\left[\left(\hat{m}_q\right)^2\right] = \left.\frac{d^2M}{d\theta^2}\right|_{\theta=0} = 2a_1^2 n\left(\frac{n}{2}+1\right) + 2a_1 a_2 n^2 + 2a_2^2 n\left(\frac{n}{2}+1\right) \tag{33}$$

All the terms like $(1-2a_i\theta)$ disappear.

The variance is:

$$Var\left(\hat{m}_q\right) = E[\left(\hat{m}_q\right)^2] - \left(E[\hat{m}_q]\right)^2 = 2n(a_1^2 + a_2^2) \tag{34}$$

The result in Eq. (32) and (34) refer to the special case $N = 2$. Generalising to any N yields:

$$E\left[\hat{m}_q\right] = n\sum_{i=1}^{N} a_i \qquad Var\left(\hat{m}_q\right) = 2n\sum_{i=1}^{N} a_i^2 \tag{35}$$

which coincides with Eq. (22).

References

1 Miles JW. On structural fatigue under random loading. J Aeron Sci 1954;21(11):753–62. https://doi.org/10.2514/8.3199

2 Bendat JS. Probability Functions for Random Responses: Prediction of Peaks, Fatigue Damage, and Catastrophic Failures. NASA-CR-33; 1964.

3 Dirlik T. Application of computers in fatigue analysis. Ph.D. thesis. UK: University of Warwick; 1985.

4 Lutes LD, Larsen CE. Improved spectral method for variable amplitude fatigue prediction. J Struct Eng-ASCE 1990;116(4):1149–1164. https://doi.org/10.1061/(ASCE)0733-9445(1990)116:4(1149)

5 Larsen CE, Lutes LD. Predicting the fatigue life of offshore structures by the single-moment method. Probab Eng Mech 1991;6(2):96–108. https://doi.org/10.1016/0266-8920(91)90023-W

6 Benasciutti D, Tovo R. Comparison of spectral methods for fatigue analysis of broad-band Gaussian random processes. Probab Eng Mech 2006;21(4):287–299. https://doi.org/10.1016/j.probengmech.2005.10.003

7 Larsen CE, Irvine T. A review of spectral methods for variable amplitude fatigue prediction and new results. Procedia Engineering 2015;101:243–250. https://doi.org/10.1016/j.proeng.2015.02.034

8 Niesłony A, Böhm M, Łagoda T, Cianetti F. The use of spectral method for fatigue life assessment for non-Gaussian random loads. Acta Mechanica et Automatica 2016;10(2):100–103. https://doi.org/10.1515/ama-2016-0016

9 Benasciutti D, Tovo R. Frequency-based analysis of random fatigue loads: Models, hypotheses, reality. Materialwiss Werkstofftech 2018;49(3):345–367. https://doi.org/10.1002/mawe.201700190

10 Böhm M. Fatigue life assessment with the use of spectral method for materials subjected to standardized wind loading spectrums. AIP Conference Proceedings 2018;2029:020005. https://doi.org/10.1063/1.5066467

11 Roberts JB. Structural fatigue under non-stationary random loading. J Mech Eng Sci 1966;8(4):392-405. https://doi.org/10.1243/JMES_JOUR_1966_008_051_02

12 Benasciutti D, Tovo R. Frequency-based fatigue analysis of non-stationary switching random loads. Fatigue Fract Eng Mater Struct 2010;30(11):1016–1029. https://doi.org/10.1111/j.1460-2695.2007.01171.x

13 Trapp A, Makua MJ, Wolfsteiner P. Fatigue assessment of amplitude-modulated non-stationary random vibration loading. Procedia Structural Integrity 2019;17:379-386. https://doi.org/10.1016/j.prostr.2019.08.050

14 Bendat JS, Piersol AG. Random data: analysis and measurement procedures. 4th ed. New York: John Wiley & Sons; 2010.

15 Chakrabarti SK, Cooley RP. The stability of some currently used wave parameters – A discussion. Coast Eng 1977;1:359–365. https://doi.org/10.1016/0378-3839(77)90023-0

16 Donelan M, Pierson WJ. The sampling variability of estimates of spectra of wind-generated

gravity waves. J Geophys Res-Oceans 1983; 88(C7):4381–4392. https://doi.org/10.1029/JC088iC07p04381

17 Young IR. Probability distribution of spectral integrals. J Waterw Port Coast Ocean Eng 1986;112(2):338–341. https://doi.org/10.1061/(ASCE)0733-950X(1986)112:2(338)

18 Young IR. The determination of confidence limits associated with estimates of the spectral peak frequency. Ocean Eng 1995;22(7):669–686. https://doi.org/10.1016/0029-8018(95)00002-3

19 Rodríguez G, Guedes SoaresC, Machado U. Uncertainty of the sea state parameters resulting from the methods of spectral estimation. Ocean Eng 1999;26(10):991–1002. https://doi.org/10.1016/S0029-8018(98)00027-4

20 Benasciutti D. The role of uncertainty of power spectral density data in estimating the fatigue damage of random uniaxial loadings through frequency-domain methods. In: Proceedings of the Fourth International Conference on Material and Component Performance under Variable Amplitude Loading (VAL4), scheduled from 30 March to 1 April 2020 in Darmstadt, Germany, Publisher: DVM, Berlin, Germany, pp. 91–100.

21 Rice SO. Mathematical analysis of random noise, Part 1 and 2. Bell System Technical Journal 1944;23(3):282-332. https://doi.org/10.1002/j.1538-7305.1944.tb00874.x

22 Lutes LD, Sarkani S. Random Vibrations: Analysis of Structural and Mechanical Systems. 2nd ed. Burlington: Elsevier Butterworth–Heinemann; 2004.

23 Wirsching PH, Paez TL, Ortiz K. Random vibrations: theory and practice. New York: John Wiley & Sons; 1995.

24 Berger C, Eulitz K-G, Heuler P, Kotte K-L, Naundorf H, Schuetz W, Sonsino CM, Wimmer A, Zenner H. Betriebsfestigkeit in Germany – an overview. Int J Fatigue 2002;24(6):603–625. https://doi.org/10.1016/S0142-1123(01)00180-3

25 FKM Guideline. Analytical strength assessment of components in mechanical engineering, 5th ed., FKM, Frankfurt, 2003.

26 ISO 8608: 1995, Mechanical vibration – Road surface profiles – Reporting of measured data, International Organization for Standardization, 1995.

27 Pierson WJ, Moskowitz L. A proposed spectral form for fully developed wind seas based on the similarity theory of S. A. Kitaigorodskii. J Geophys Res 1964;69(24): 5181–5190. https://doi.org/10.1029/JZ069i024p05181

28 Holmes JD, Wind loading of structures (2nd ed.), Taylor & Francis, Abingdon, UK, 2007.

29 Welch PD. The use of fast Fourier transform for the estimation of power spectra: A method based on time averaging over short modified periodograms. IEEE Trans Audio Electroacoustics 1967;AU-15(2):70–73. https://doi.org/ 10.1109/TAU.1967.1161901

30 Niesłony A, Böhm M, Materac A. Influence of estimation methods of power spectral density function on the calculated fatigue life with spectral method. Solid State Phenom 2015;224:118–123. https://doi.org/10.4028/www.scientific.net/SSP.224.118

31 Montgomery DC, Runger GC. Applied statistics and probability for engineers. 6th ed. Hoboken, NJ, USA: John Wiley & Sons; 2014.

32 Lalanne C. Random Vibration: Mechanical Vibration and Shock Analysis (vol. 3). 3rd ed.

Hoboken: John Wiley & Sons; 2014.

33 Richards D. Hibbert B. A round robin exercise on road transportation data. Journal of the IEST 1993;36(4):19–27. https://doi.org/10.17764/jiet.2.36.4.166473405m520718CEES

34 Rouillard V. Quantifying the non-stationarity of vehicle vibrations with the run test. Packag Technol Sci 2014;27(3):203-219. https://doi.org/10.1002/pts.2024

35 Feiveson AH, Delaney FC. The distribution and properties of a weighted sum of chi squares. NASA Technical note NASA TN D-4575, 1968.

36 Moschopoulos PG, Canada WB. The distribution function of a linear combination of chi-squares. Comput Math Appl 1984;10(4/5): 383-386. https://doi.org/10.1016/0898-1221(84)90066-X

37 Koopmans LH. The spectral anlaysis of time series. San Diego, CA: Academic press; 1995.

38 Jenkins GM, Watts DG. Spectral anlaysis and its applciation. San Francisco, CA: Holden-Day; 1968

39 Wirsching PH, Preasthofer PH. Preliminary dynamic assessment of deepwater platforms. J Struct Division ASCE 1976;102(7):1447-62.

Funding

This research did not receive any specific grant from funding agencies in the public, commercial, or not-for-profit sectors.

TABLES

Table 1. Parameters used in numerical simulations, showing the relationship between block number, frequency resolution, standard error and total time length. Overlap fraction is $\boldsymbol{r = 0.50}$ and $\boldsymbol{r = 0.75}$.

Number of segments, K	**dof, $n = 2K$**	**Standard error, ε_r**	**Frequency resolution, Δf [Hz]**	**Segment length, T_s [s]**	**Total length, T [s]**		**Estimated confidence, $\hat{\alpha}$**
					$r = 0.50$	$r = 0.75$	
5	10	0.447	0.005	200	600	400	0.969
			0.01	100	300	200	0.969
			0.02	50	150	100	0.963
			0.03	33	100	67	0.962
15	30	0.258	0.005	200	1600	900	0.956
			0.01	100	800	450	0.959
			0.02	50	400	225	0.959
			0.03	33	267	150	0.953
35	70	0.169	0.005	200	3600	1900	0.951
			0.01	100	1800	950	0.952
			0.02	50	900	475	0.952
			0.03	33	600	317	0.952
75	150	0.115	0.005	200	7600	3900	0.951
			0.01	100	3800	1950	0.952
			0.02	50	1900	975	0.950
			0.03	33	1267	650	0.951

FIGURE CAPTIONS

Figure 1. (a) Sample record and segments; (b) true and estimated PSD with confidence interval.

Figure 2. Equivalent degrees of freedom υ_0 as a function of the PSD shape (Δf=0.1 Hz, f_{max}=55 Hz, N=551). The boxes indicate the values of υ_0.

Figure 3. Comparison between the true power spectra density and two sample realisations obtained for different combinations of n and Δf.

Figure 4. Probability density function of the sample 'single-moment' damage (normalised to the expected damage), as a function of the sixteen combinations of frequency resolution and dofs.

Figure 5. Normal probability plot of the sample 'single-moment' damage for two different combinations: (a) n=10, Δf=0.03 Hz, (b) n=150, Δf=0.005 Hz.

Figure 6. Sample of 25 confidence intervals constructed around the sample damage and compared with the 'true' damage (horizontal line). Results refer to: (a) n=10, Δf=0.03 Hz; (b) n=70, Δf=0.01 Hz.

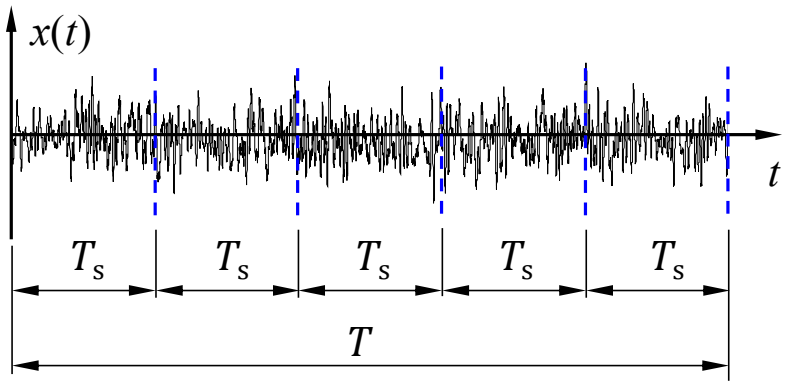

(a)

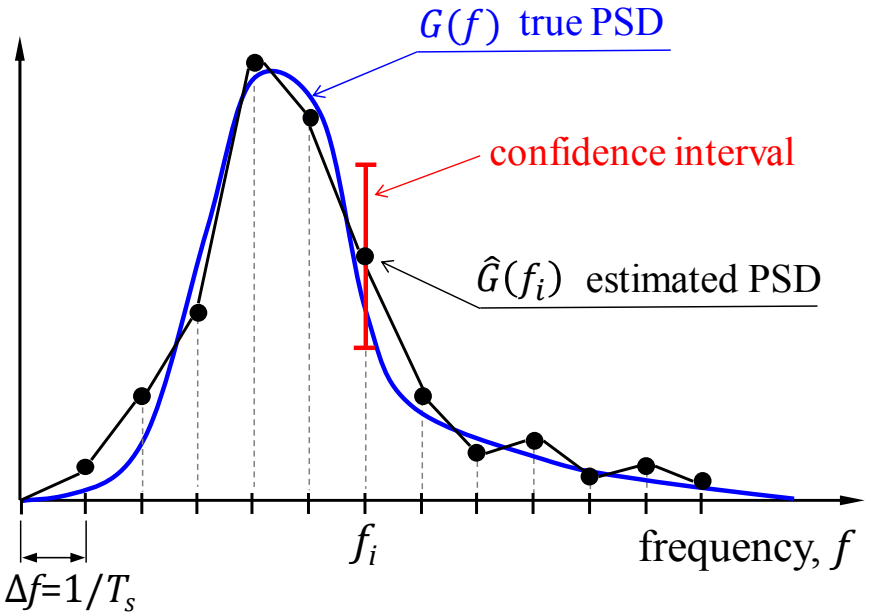

(b)

Figure 1. (a) Sample record subdivided into disjoint segments; (b) true PSD, estimated PSD and confidence interval.

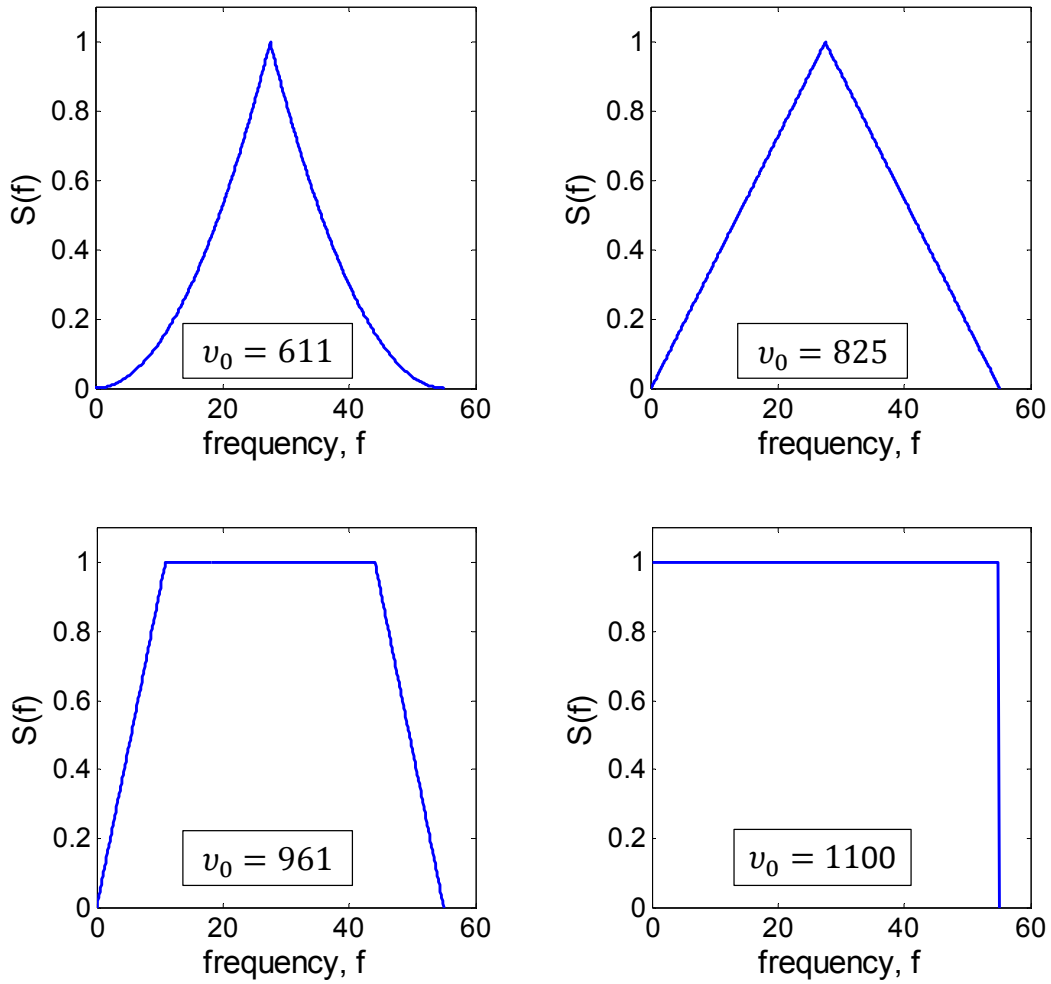

Figure 2. Equivalent degrees of freedom υ_0 as a function of the PSD shape (Δf=0.1 Hz, f_{max}=55 Hz, N=551). The boxes indicate the values of υ_0.

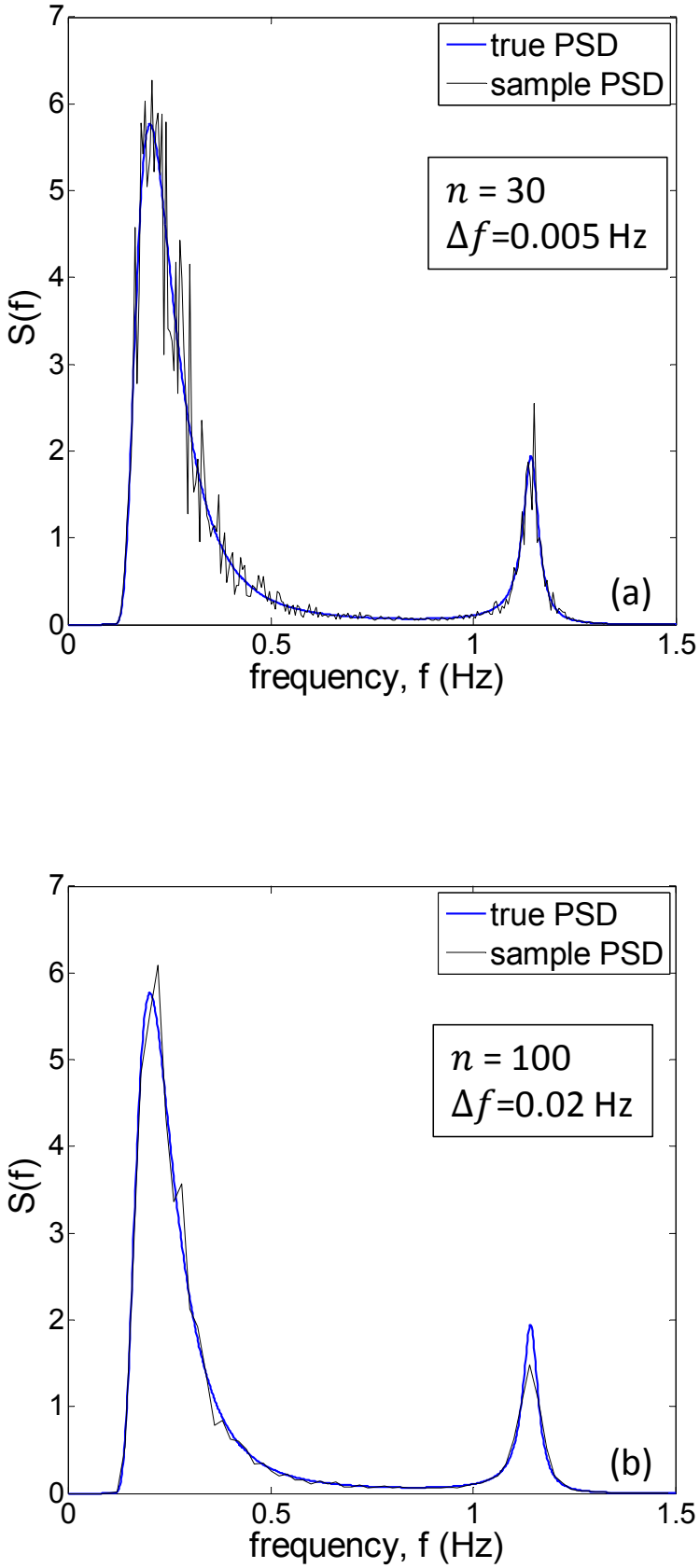

Figure 3. Comparison between the true power spectra density and two sample realisations obtained for different combinations of n and Δf.

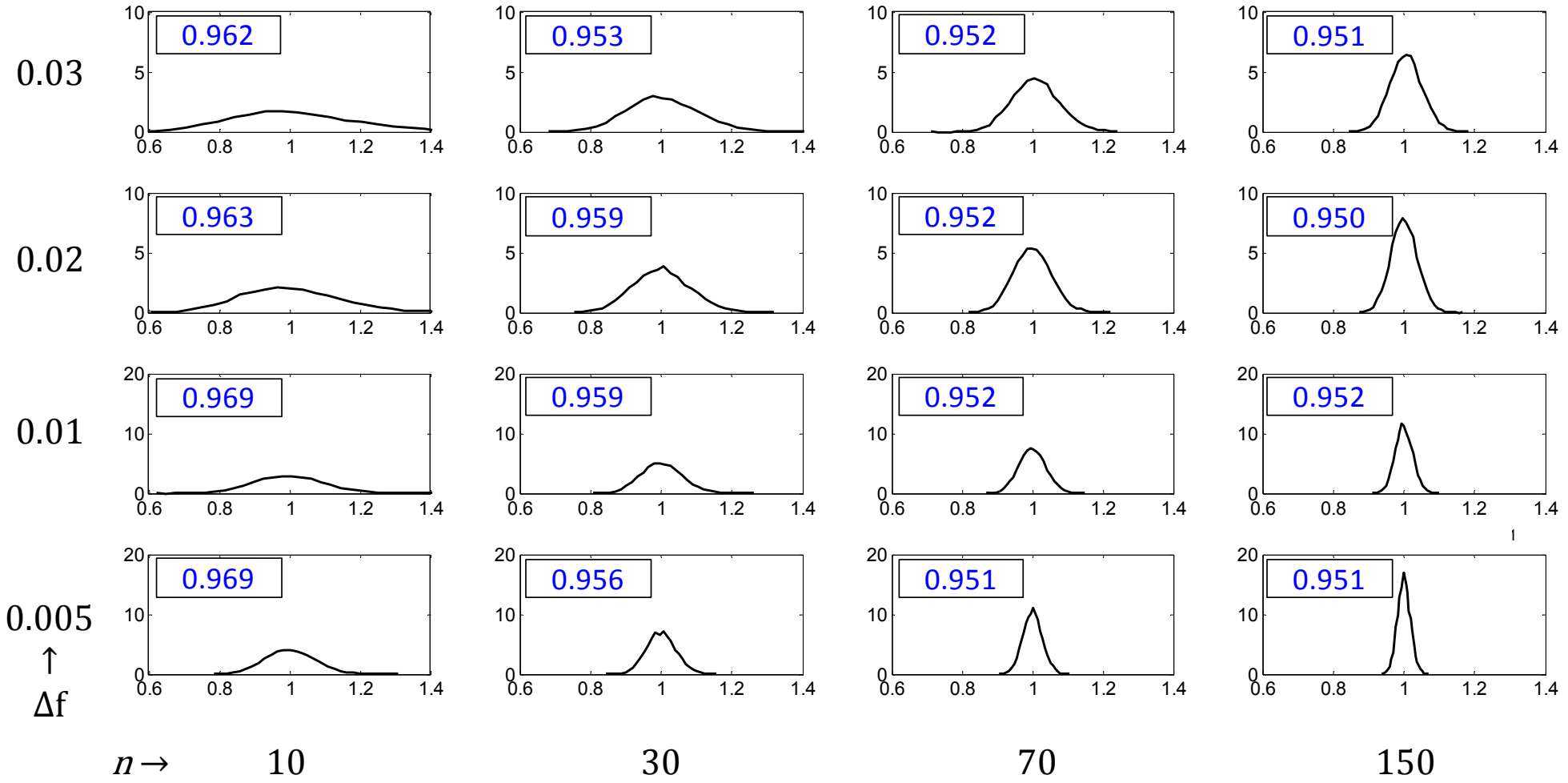

Figure 4. Probability density function of the sample 'single-moment' damage (normalised to the expected damage), as a function of the sixteen combinations of frequency resolution and dofs.

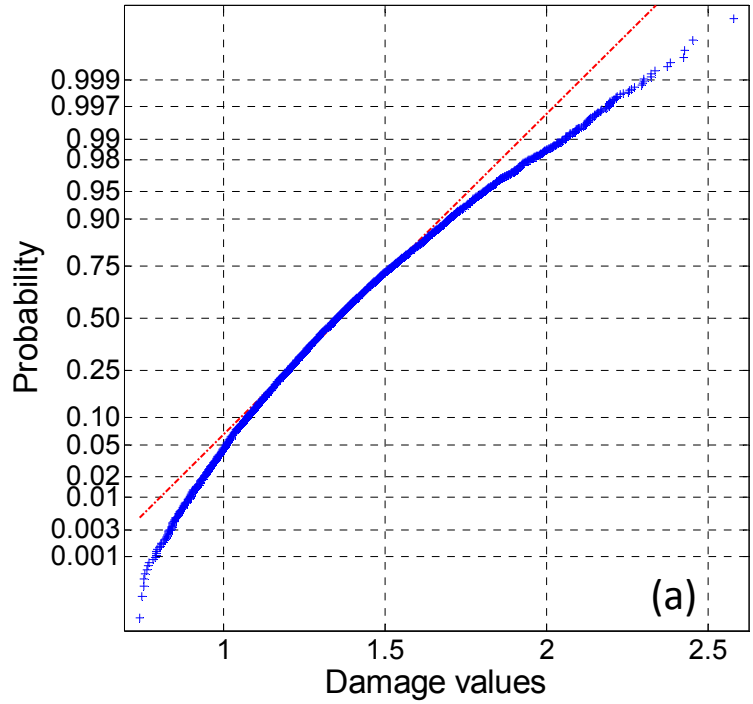

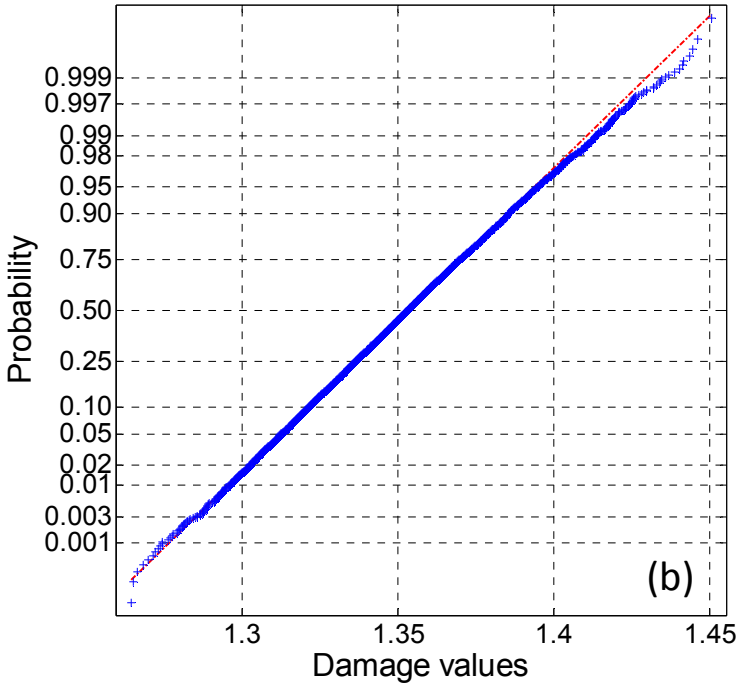

Figure 5. Normal probability plot of the sample 'single moment' damage for two different combinations: (a) n=10, Δf=0.03 Hz, (b) n=150, Δf=0.005 Hz.

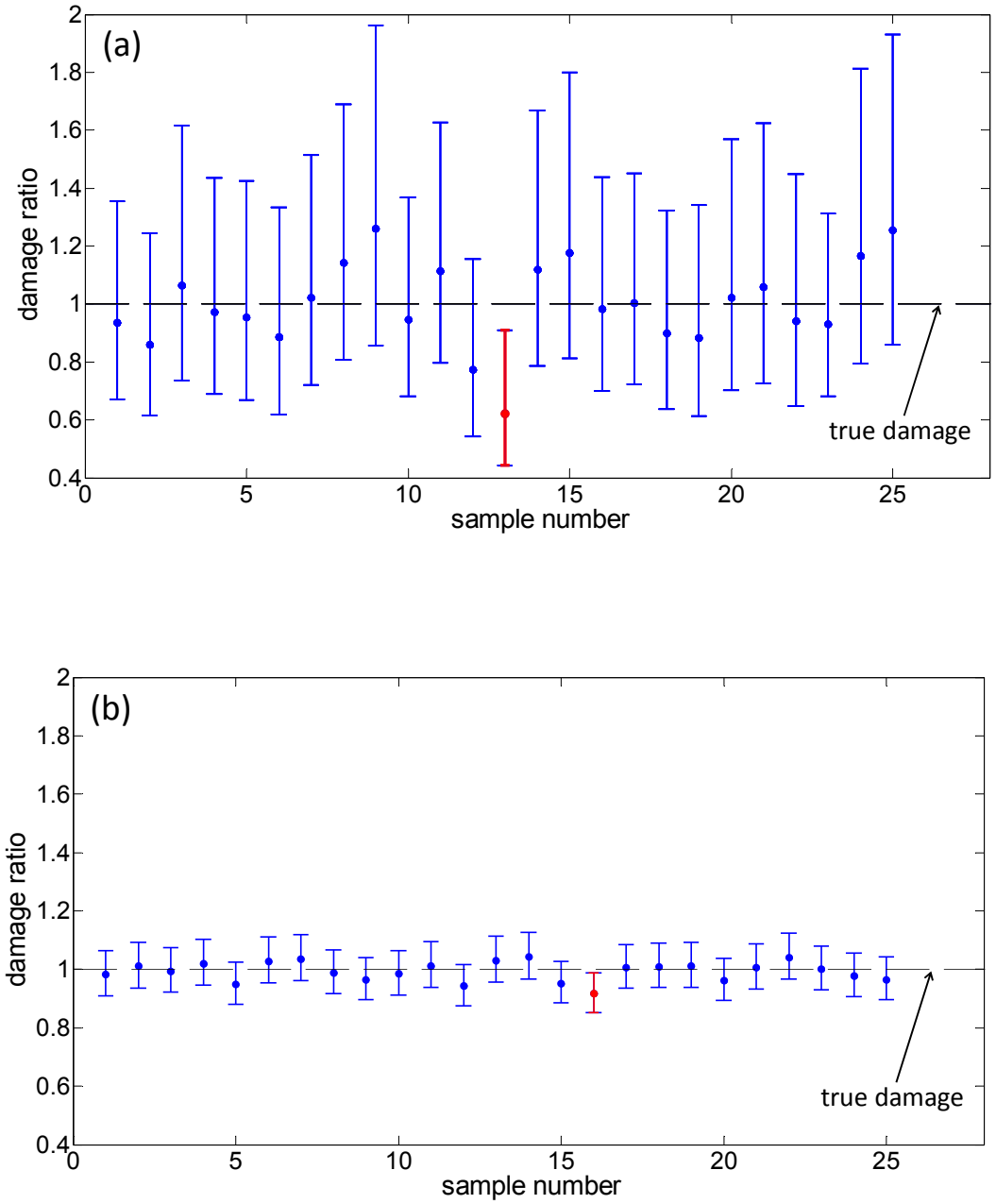

Figure 6. Sample of 25 confidence intervals constructed around the sample damage and compared with the 'true' damage (horizontal line). Results refer to: (a) n=10, Δf=0.03 Hz; (b) n=70, Δf=0.01 Hz.